ACS Catalysis

Research Article

pubs.acs.org/acscatalysis

Electron Transfer Mediator Effects in the Oxidative Activation of a Ruthenium Dicarboxylate Water Oxidation Catalyst

Matthew V. Sheridan, Benjamin D. Sherman, Zhen Fang, Kyung-Ryang Wee, Michael K. Coggins, and Thomas J. Meyer*

Department of Chemistry, University of North Carolina at Chapel Hill, Chapel Hill, North Carolina 27599, United States

Supporting Information

ABSTRACT: The mechanism of electrocatalytic water oxidation by the water oxidation catalyst, ruthenium 2,2′-bipyridine-6,6′-dicarboxylate (bda) bis-isoquinoline (isoq), [Ru(bda)(isoq)$_2$], **1**, at metal oxide electrodes has been investigated. At indium-doped tin oxide (ITO), diminished catalytic currents and increased overpotentials are observed compared to glassy carbon (GC). At pH 7.2 in 0.5 M $NaClO_4$, catalytic activity is enhanced by the addition of $[Ru(bpy)_3]^{2+}$ (bpy = bipyridine) as a redox mediator. Enhanced catalytic rates are also observed at ITO electrodes derivatized with the surface-bound phosphonic acid derivative $[Ru(4,4'\text{-}(PO_3H_2)_2bpy)(bpy)_2]^{2+}$, **RuP**$^{2+}$. Controlled potential electrolysis with measurement of O_2 at ITO with and without surface-bound RuP^{2+} confirm that water oxidation catalysis occurs. Remarkable rate enhancements are observed with added acetate and phosphate, consistent with an important mechanistic role for atom-proton transfer (APT) in the rate-limiting step as described previously at GC electrodes.

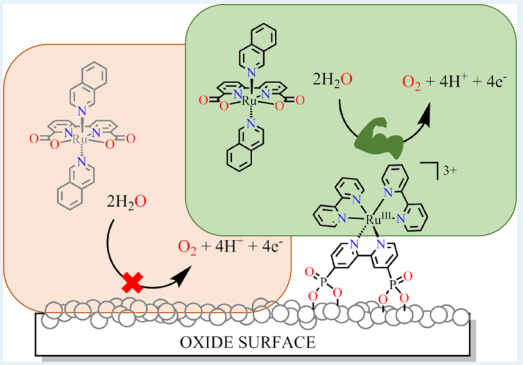

KEYWORDS: *water oxidation, electrocatalysis, electron transfer, polypyridyl ruthenium complexes, water splitting*

1. INTRODUCTION

Water oxidation catalysis by Ru(II) polypyridyl-aqua complexes has played a major role in the ongoing effort to make solar fuels by artificial photosynthesis.[1] The advantages of these ruthenium-based catalysts include their availability and coordinative stability in multiple oxidation states from Ru(II) to Ru(V) with polypyridyl ligands. Oxidative activation to $Ru^{IV}{=}O^{2+}$ occurs by proton coupled electron transfer (PCET) – $Ru^{II}{-}OH_2^{2+} \xrightarrow{-e^-,-H^+} Ru^{III}{-}OH^{2+} \xrightarrow{-e^-,-H^+} Ru^{IV}{=}O^{2+}$ – followed by further oxidation to $Ru^{V}(O)^{3+}$ – $Ru^{IV}{=}O^{2+} \xrightarrow{-e^-} Ru^{V}(O)^{3+}$.[2] The accessibility of multiple oxidation states without significant charge buildup provides a basis for accumulating multiple oxidative equivalents at a single site for water oxidation, eq 1. The well-defined redox chemistry of these Ru(II) polypyridyl complexes makes them particularly amenable to mechanistic studies based on electrochemical oxidation or oxidation by Ce^{IV} in acidic solutions.[2]

$$2H_2O \rightarrow O_2 + 4H^+ + 4e^- \quad (1)$$

Recently, Sun and co-workers have made a significant advance in this area in developing neutral $Ru^{II}(bda)(L)_2$ (bda = 2,2′-bipyridine-6,6′-dicarboxylate, L = isoquinoline (isoq), **1**, picoline, **2**) catalysts (Scheme 1).[3] They have dramatically increased catalytic activities at lower overpotentials than for previously reported Ru(II) polypyridyl complexes.

Results of mechanistic studies on catalysts **1** and **2** are available from UV–vis kinetic measurements in acidic solutions with Ce^{IV} as the oxidant, supported by computational studies.[4] They reveal the mechanism in Scheme 2[4] in which oxidation to Ru(V) is followed by rate-limiting O···O coupling to give a $Ru^{IV,IV}(\eta^1{:}\eta^1\text{-}O_2)$ bridged intermediate and oxygen evolution. A recent report has suggested a possible important role for a $Ru^{III}{-}O{-}Ru^{III}$ intermediate based on spectroelectrochemical data.[5]

The results of mechanistic studies on a series of Ru(II) polypyridyl aqua complexes have revealed single-site pathways with O atom transfer from $Ru^{V}(O)$ or $Ru^{IV}(O)$ to a water molecule with concerted proton transfer to the solvent or an added base (B), by atom-proton transfer (APT), Scheme 3.[6] Evidence has been found in these cycles for peroxide intermediates (Scheme S1 in the Supporting Information).[7,8]

Electrochemical measurements have been used to obtain pH-dependent redox potential data for the $Ru^{II}(bda)(L)_2$ couples involved in water oxidation.[4,9,10] Recently, we reported the results of an in-depth study on $Ru^{II}(bda)(isoq)_2$ which gave added insights into both the coordination chemistry and water oxidation catalysis by **1** at glassy carbon (GC) electrodes.[11] The results of that study were consistent with single-site water oxidation with no direct evidence for a second-order pathway.[4,12] Remarkably high rates of water oxidation were observed with added buffer bases and attributed to atom-proton transfer (APT) pathways, Scheme 3.[6c]

Received: April 6, 2015
Revised: May 26, 2015
Published: June 9, 2015

DOI: 10.1021/acscatal.5b00720
ACS Catal. 2015, 5, 4404–4409

Scheme 1. Metal Complexes of Interest

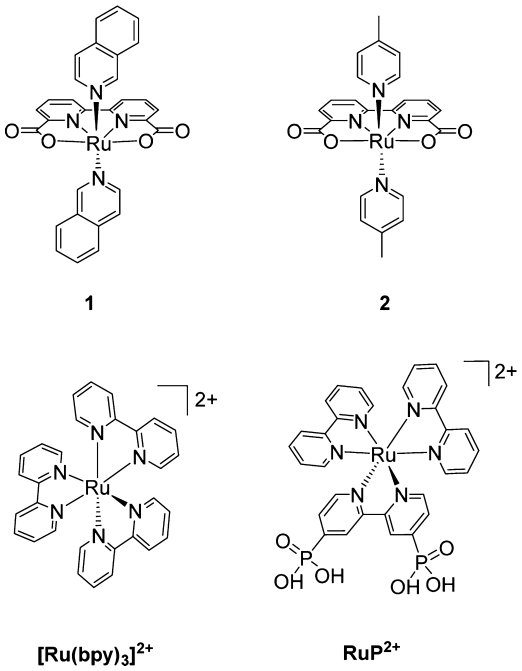

Scheme 2. Proposed Water Oxidation Cycle for 1 (Ref 4)

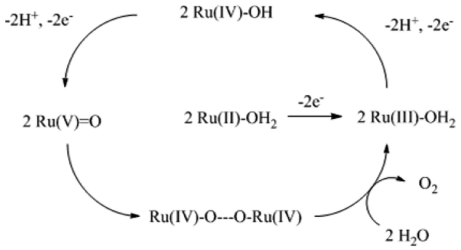

Scheme 3. (Top) Atom-Proton Transfer (APT) Pathway for a Single-Site $[Ru^{V}(O)]^{3+}$ Oxidant (Ref 6c); (Bottom) Mechanism for APT Water Oxidation by 1 with HPO_4^{2-} as the Added Buffer Base at Glassy Carbon

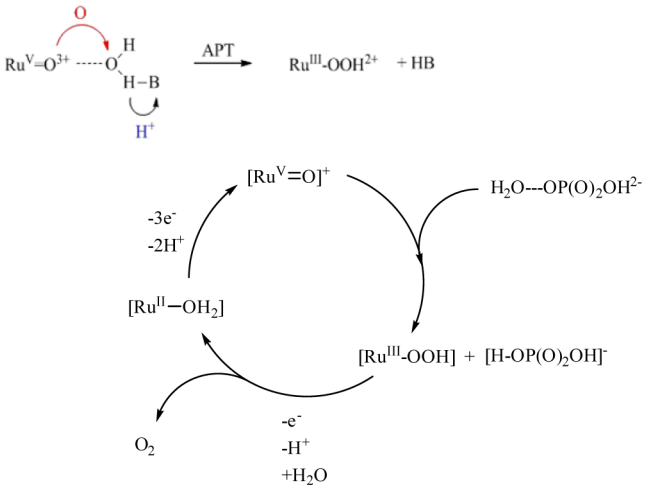

We report here on the results of a related study on water oxidation electrocatalysis by **1**. They highlight the importance of specific electrode effects, electron transfer mediation, and APT pathways in catalyzing water oxidation at indium-doped tin oxide (ITO) electrodes.[13]

2. EXPERIMENTAL SECTION

Materials. All commercial chemical reagents were used as received. All solutions were freshly prepared with deionized water provided by a Milli-Q purification system (Synthesis A10) and were purged with nitrogen to remove O_2 before electrochemical experiments. Compounds **1**, **2**, and **RuP**$^{2+}$ were prepared according to literature methods.[4,14] $[Ru(bpy)_3]^{2+}$ was obtained commercially as the chloride salt (Sigma).

Electrochemistry. Electrochemical measurements were performed with a CH Instruments 660D electrochemical workstation at room temperature. A three-electrode configuration was applied in a single compartment cell with glassy carbon (GC) and boron-doped diamond (BDD) (d = 3 mm, A = 0.071 cm^2) working electrodes, Ag/AgCl (3 M NaCl, 0.21 V vs NHE) and saturated calomel electrodes (SCE, 0.24 V vs NHE) used as reference electrodes, and platinum wire counter electrode. GC and BDD electrodes were polished with 1 μm MicroPolish alumina powder (Buehler, Inc.). Solutions were purged with nitrogen through a solvent bubbler filled with Milli-Q H_2O in order to exclude O_2, reduce evaporation, and to prevent catalyst decomposition. Planar fluorine-doped tin oxide (ITO) on glass (Hartford Glass; sheet resistance =15 Ω/sq.) was also employed. The ITO substrate was modified with surface absorbed mediator, **RuP**$^{2+}$.

Surface coverages for **RuP**$^{2+}$, Γ in mol/cm^2, were evaluated from the integrated current under voltammetic waves to give the coulombs based, Q, by using the expression, $\Gamma = Q \times (F \times A \times n)^{-1}$. In this expression, F is Faraday's constant, 96 485 C/mol, A the electrode area in cm^2, and n is the number of electrons passed with n = 1 for **RuP**$^{2+}$.[15]

3. RESULTS AND DISCUSSION

Figure 1 shows cyclic voltammograms (CV) for **1** at GC and ITO electrodes in pH 7.2 aqueous solutions 10% by volume in acetonitrile (MeCN) and 0.5 M $NaClO_4$. Under these conditions, MeCN is coordinated to the Ru(II) form of the catalyst, Scheme 4, with pK_a = 2.4 for the open-arm −COOH chelate.[11] The first quasi-reversible wave at $E_{1/2}$ = 0.62 V vs the saturated calomel electrode (SCE; 0.24 V vs NHE) arises from a 2e$^-$/2H$^+$ Ru$^{IV/II}$ couple at this pH.[16] Oxidation of the Ru(II) form of the complex is accompanied by exchange of

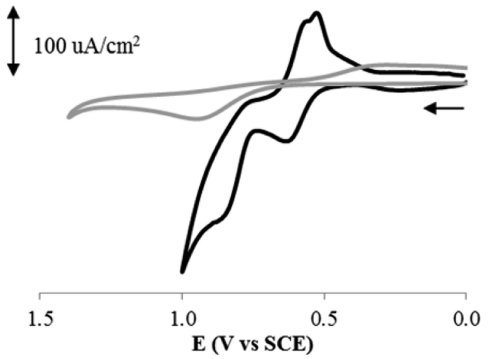

Figure 1. CVs of 0.25 mM 1 in a pH 7.2 solution with 10% MeCN (v/v) and 0.5 M $NaClO_4$ with background subtraction at GC (black) and ITO electrodes (gray); scan rate = 0.1 V/s.

DOI: 10.1021/acscatal.5b00720
ACS Catal. 2015, 5, 4404−4409

Scheme 4. Electrochemical Oxidation of 1 in a pH 7.2 Solution with 10% MeCN (v/v) and 0.5 M $NaClO_4$

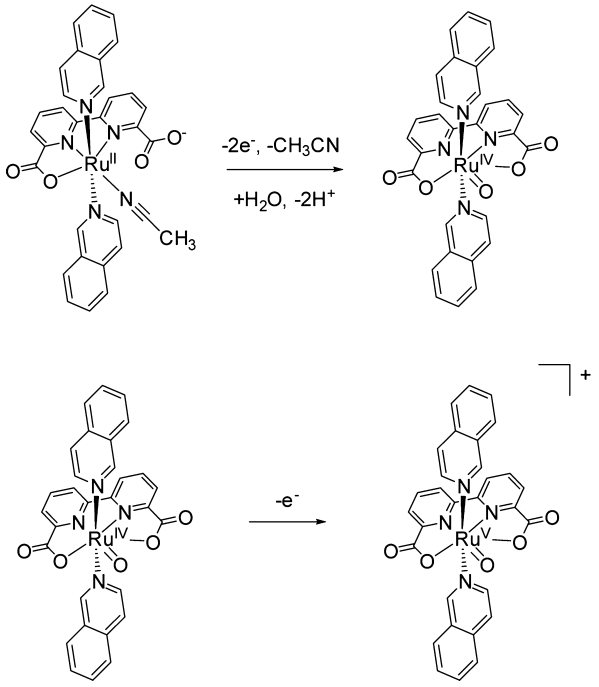

coordinated MeCN for water followed by proton loss and oxo formation, Scheme 4.

The first oxidation wave for **1** at ITO is highly distorted with peak potentials at $E_{p,ox}$ = 0.94 V and $E_{p,red}$ = 0.30 V and ΔE_p = 0.64 V, consistent with kinetically inhibited electron transfer at the electrode. Under the same conditions, ΔE_p = 60 mV at glassy carbon (GC). Inhibition to oxidation at oxide electrodes in water has been observed for neutral organics and attributed to inhibited diffusion through the highly ordered double layer in water at the electrode−solution interface.[17]

While there is no evidence for significant electrocatalytic water oxidation at ITO, or for a well-defined wave for Ru(IV) oxidation to Ru(V), at GC a catalytic onset for water oxidation does occur just past the $Ru^{V/IV}$ wave at $E_{1/2}$ = 0.78 V in 10% MeCN/H_2O at pH 7.2, 0.5 M in $NaClO_4$. Based on the results of the earlier study, the proposed mechanism for water oxidation is shown in eqs 1-4 with the O···O bond-forming step illustrated in the bottom of Scheme 3.[11]

$$[Ru^{II}(MeCN)] + H_2O \xrightarrow{-2e^-,2H^+} [Ru^{IV}(O)] + MeCN \quad (1)$$

$$[Ru^{IV}(O)] \xrightarrow{-e^-} [Ru^{V}(O)]^+ \quad (2)$$

$$[Ru^{V}(O)]^+ + H_2O \rightarrow [Ru^{III}(OOH)] + H^+ \quad (3)$$

$$[Ru^{III}(OOH)] \xrightarrow{-4e^-,+H_2O,-3H^+} [Ru^{V}(O)]^+ + O_2 \quad (4)$$

Evidence for the buildup of a $[Ru^{III}(OOH)]$ intermediate following an oxidative scan through the water oxidation wave is observed in the CVs in Figure 1 as an additional, irreversible rereduction wave at $E_{p,c}$ = 0.53 V. An analogous wave appears at $E_{p,c}$ = 0.29 V for complex **2** at a boron-doped diamond (BDD) electrode, Figure 2. The shift to a more negative potential for rereduction of the "hydroperoxide" of **2** compared to **1** is consistent with the more electron rich axial picoline ligands in **2**.

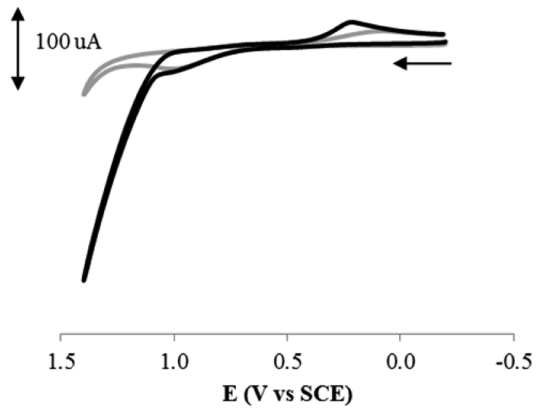

Figure 2. CV of 0.2 mM **2** in a pH 7.2 solution with 10% MeCN (v/v) and 0.5 M $NaClO_4$/3.0 mm BDD electrode, scan rate = 0.1 V/s.

Slow oxidation at the electrode and inhibited water oxidation catalysis at metal oxide electrodes has been observed for other Ru(II) polypyridyl catalysts.[18] For the "blue dimer",[19] *cis,cis*-$[(bpy)_2(H_2O)Ru^{III}ORu^{III}(H_2O)(bpy)_2]^{4+}$, rate-limiting oxidation of $[(HO)Ru^{IV}ORu^{III}(OH_2)]^{4+}$ to $[(HO)Ru^{IV}ORu^{IV}(OH)]^{4+}$ kinetically inhibits overall water oxidation both with Ce^{IV} as the oxidant and electrochemically.[20] Addition of the redox mediators $[Ru(bpy)_2(L-L)]^{2+}$, L−L = bipyridine, bipyrimidine, or bipyrazine) has been shown to promote Ce(IV) water oxidation catalysis by the blue dimer in solution[20a] and at oxide surfaces by the surface-bound phosphonic acid derivative, $[Ru(4,4'-(PO_3H_2CH_2)-bpy)_2(bpy)]^{2+}$ ($\mathbf{Ru(CH_2P)_2}^{2+}$).[20b] Cooperative redox mediator effects have also been demonstrated in chromophore-catalyst assemblies[21] and for single-site Ru(II) polypyridyl catalysts.[22] The origin of the mediator effect lies in the rapid electron transfer characteristics of the mediator couples with self-exchange rate constants for $[Ru(bpy)_3]^{3+/2+}$ in the range of $10^8 - 10^9$ s^{-1}.[23]

We investigated the role of possible mediator effects in the oxidation of **1** at ITO electrodes by both $[Ru(bpy)_3]^{2+}$ as a diffusional mediator and by $\mathbf{RuP}^{2+}$ on ITO, ITO−$\mathbf{RuP}^{2+}$. In solutions containing both **1** (0.25 mM) and $[Ru(bpy)_3]^{2+}$ (0.25 mM), a significant increase in current arising from water oxidation catalysis occurs at the potential for the $[Ru(bpy)_3]^{3+/2+}$ couple at $E_{1/2}$ = 1.06 V. Addition of the redox mediator leaves the wave for the $Ru^{IV/II}$ couple relatively unaffected. Under these conditions, water oxidation is enhanced by $[Ru(bpy)_3]^{3+/2+}$ mediator oxidation of Ru^{IV} to Ru^{V} followed by water oxidation (black line, Figure 3). In a previous study, $[Ru(bpy)_3]^{2+}$ was used as a photosensitizer for water oxidation catalysis by **2**.[24] In our experiments, there is no evidence for water oxidation catalysis by $[Ru(bpy)_3]^{2+}$ in the absence of **1** with the reversible $[Ru(bpy)_3]^{3+/2+}$ couple appearing in CVs at 1.06 V (Figure S1). Current enhancements observed with added mediator increased linearly in dilute solutions and reached saturation above 0.25 mM in added $[Ru(bpy)_3]^{2+}$ (Figure S2) under conditions where water oxidation by Ru^{V} became rate-limiting.

Ratios of catalytic (i_{cat}) to peak (i_p) currents for the $Ru^{IV/II}$ couple were compared as a measure of relative rates of water oxidation. From the data in Figure 3, i_{cat}/i_p values at 1.4 V were

DOI: 10.1021/acscatal.5b00720
ACS Catal. 2015, 5, 4404−4409

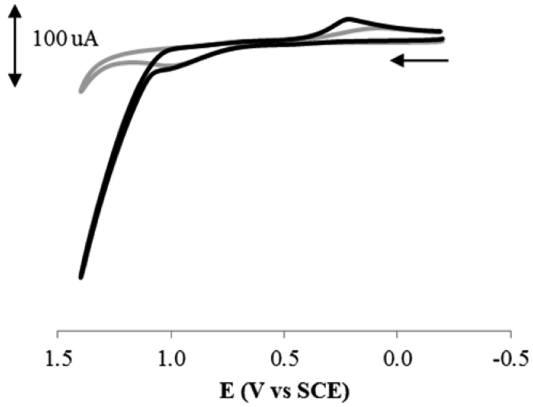

Figure 3. CVs of 0.25 mM **1** in a pH 7.2 solution with 10% MeCN (v/v) and 0.5 M $NaClO_4$ at a 1 cm^2 planar ITO electrode with (black) and without (gray) 0.25 mM $[Ru(bpy)_3]^{2+}$.

10.4 and 2.0 with and without added $[Ru(bpy)_3]^{2+}$, a current enhancement ~5. The added mediator also decreased the overpotential for water oxidation by 275 mV, based on the potential needed to reach the i_{cat}/i_p value for **1** at 1.4 V without added $[Ru(bpy)_3]^{2+}$.

As described previously, ITO−$\mathbf{RuP}^{2+}$ slides were prepared by soaking in a 10^{-4} M methanol solution of $[\mathbf{RuP}^{2+}][ClO_4]_2$ for 2 h giving a monolayer surface coverage of ~1.2×10^{-10} mol/cm^2 as determined by integration of the ITO−$\mathbf{RuP}^{3+/2+}$ wave in Figure 4.[15] As shown in Figure 4, derivatization of ITO by

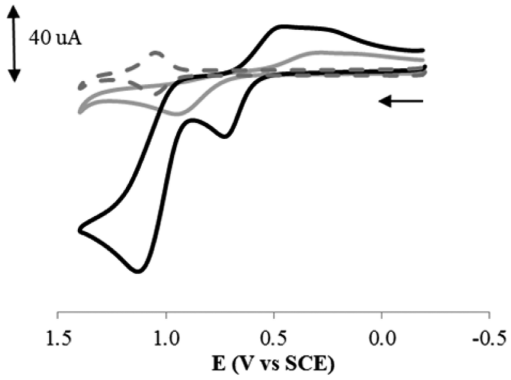

Figure 4. CVs of 0.25 mM **1** in a pH 7.2 solution with 10% MeCN (v/v) and 0.5 M $NaClO_4$ at a 1 cm^2 planar ITO electrode with (black) and without (gray) surface-bound $\mathbf{RuP}^{2+}$ (ITO−$\mathbf{RuP}^{2+}$) at 0.1 V/s. The surface-bound $\mathbf{RuP}^{2+}$ (ITO−$\mathbf{RuP}^{2+}$) in the absence of catalyst under the same conditions (dotted gray).

−$\mathbf{RuP}^{2+}$ also resulted in mediated current enhancement of the solution $Ru^{V/IV}$ wave, eq 5, and enhanced electrocatalytic water oxidation.

$$\text{ITO} - \mathbf{RuP}^{2+} \xrightarrow{-e^-} \text{ITO} - \mathbf{RuP}^{3+} \quad (5)$$

$$\text{ITO} - \mathbf{RuP}^{3+} + [Ru^{IV}(O)] \rightarrow \text{ITO} - \mathbf{RuP}^{2+} + [Ru^{V}(O)]^+ \quad (6)$$

For Ru(II) polypyridyl aqua complexes such as $[Ru(Mebimpy)(bpy)(OH_2)]^{2+}$ [Mebimpy = 2,6-bis(1-methylbenzimidazol-2-yl)pyridine; bpy = 2,2′-bipyridine], significant rate accelerations are typically observed with added proton acceptor bases− $H_2PO_4^-$, $CH_3CO_2^-$, HPO4^2—an effect attributed to rate-limiting O···O bond formation by Atom Proton Transfer (APT), top of Scheme 3.[6c,7] A possible role for mediated APT in water oxidation catalysis by **1** was investigated at ITO−$\mathbf{RuP}^{2+}$ with added $H_2PO_4^-/HPO_4^{2-}$ buffer at pH 7.2 with 0.5 M $NaClO_4$. As shown by the data in Figure 5, catalytic currents increase linearly with added HPO_4^{2-} at a fixed buffer ratio of $H_2PO_4^{2-}/HPO_4^{2-}$ = 0.46.

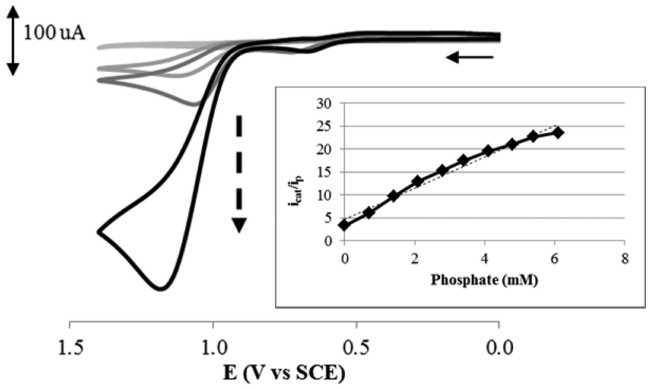

Figure 5. CVs of 0.25 mM 1 in a pH 7.2 solution with 10% MeCN (v/v) and 0.5 M $NaClO_4$ at a 1 cm^2 planar ITO electrode (gray) and at ITO−RuP^{2+} with 0.7, 1.3, and 6.1 mM added $H_2PO_4^-/HPO_4^{2-}$ buffer at a buffer ratio of 0.46 (black), all at 0.1 V/s. Inset: variation of i_{cat}/i_p with total $H_2PO_4^-/HPO_4^{2-}$ concentration.

A first-order dependence on catalyst concentration and significant rate accelerations with added proton acceptor bases are characteristic features of water oxidation by other single site Ru(II) polypyridyl catalysts by the APT pathway illustrated in Scheme 3. The O···O bond-forming mechanism at the electrode is shown in eqs 7 and 8. $H_2PO_4^-$ is expected to play a lesser role as an APT base given pK_a = 2.15 for H_3PO_4 compared to 7.20 for HPO_4^{2-}.[7] The results in Figure 5 agree with previous results found for **1** at a GC electrode.[11]

$$Ru^{IV} - O \xrightarrow{-e^-} [Ru^{V}(O)]^+ \quad (7)$$

$$[Ru^{V} - O]^+ + HOH \cdots OP(O)_2OH^{2-} \rightarrow Ru^{III}(OOH) + HOP(O)_2OH^- \quad (8)$$

A Tafel plot of log(|i|) vs potential (V) from the data in Figure 5, determined at 6.1 mM, the highest concentration of $H_2PO_4^-/HPO_4^{2-}$ buffer used in the study, at a fixed buffer ratio of 0.46, is shown in Figure 6. The slope of this plot is 129 mV/

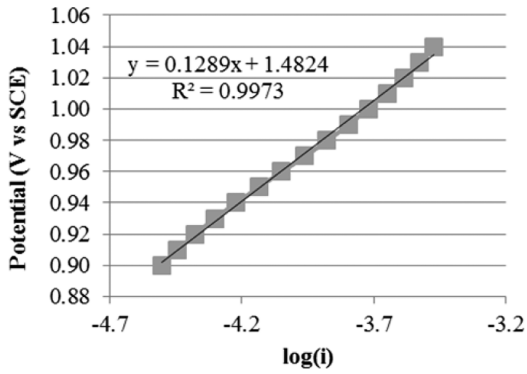

Figure 6. Tafel plot of log(|i|) vs potential (V) for the catalytic wave with 6.1 mM HPO_4^{2-} present in Figure 5, which initiates at ca. 0.9 V at pH 7.2.

DOI: 10.1021/acscatal.5b00720
ACS Catal. 2015, 5, 4404−4409

decade, in good agreement with 120 mV/decade calculated by using eq 9 for a 1e$^-$ (n = 1) electron transfer process with a transfer coefficient α, of 0.5. In eq 9, F is the Faraday constant, R the ideal gas constant, and T the temperature. The magnitude of the slope is consistent with a catalytic process rate limited by electron transfer mediation by the $-$**RuP**$^{3+/2+}$ couple.

$$\text{slope} = (2.303F^{-1}RT)/(\alpha n) \quad (9)$$

Electrocatalyzed oxygen evolution was confirmed by using a Unisense Clark-type electrode placed in the electrolysis solution. The results of three electrolysis experiments in 0.5 M $NaClO_4$ at pH 7.2 with 0.2 mM **1** are shown in Figure 7.

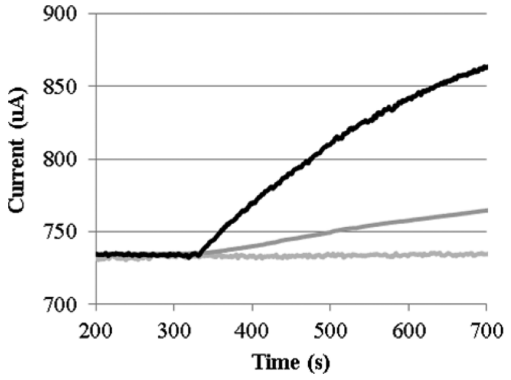

Figure 7. O_2 measurements with a Unisense probe in a pH 7.2 solution 0.2 mM in 1 and 0.5 M $NaClO_4$: at 1 cm^2 ITO$-$RuP^{2+} (dark gray) and ITO electrodes (light gray); with 8.5 mM added CH_3CO_2Na at an ITO$-$RuP^{2+} electrode (black). The initial solution was saturated with air. The results shown are for 5 min of electrolysis at 1.2 V.

Electrolysis at 1.2 V at ITO resulted in no appreciable increase in O_2 evolution. At ITO$-$**RuP**$^{2+}$, O_2 was produced with 45% Faradaic efficiency. The addition of 8.5 mM acetate dramatically increased the rate of O_2 production with the overall Faradaic efficiency rising to 80%. Acetate was used in these experiments as an APT buffer base to enhance the rate of water oxidation without significant loss of $-$**RuP**$^{2+}$ from the surface by hydrolysis (Figure S3). Electrolysis of an acetate solution for 3 h, with the total charge passed corresponding to transfer of 32 electrons per catalyst, resulted in the production of 7.4 equiv of O_2.[25] During the course of the electrolysis, the turnover number at the surface-bound heterogeneous mediator, **RuP**$^{2+}$, was 7 × 10^3 with an electron transfer turnover frequency of 8 e$^-$/sec.

As shown by the CV comparison between Figures 4 and 8, electron transfer mediation by ITO$-$**RuP**$^{2+}$ results in catalyzed current enhancements that are comparable to glassy carbon. Given the plateau or near-plateau limiting currents in Figure 8, it is possible to obtain estimates for rate constants for water oxidation by Ru^{V}(O)$^+$, k_{cat}, from i_p/i_{cat} measurements with i_p/i_{cat} related to k_{cat} as shown in eq 10. In eq 10—applied previously to water oxidation by **1** at pH 7[11]—i_p is the peak current, i_{cat} the catalytic current, and ν the scan rate (V/s).[26] However, to utilize the current ratio, it was necessary to account for inhibited diffusion in the i_p measurements arising from double layer effects. The [Ru$^{III/II}$(bda)(NCMe)(L)$_2$]$^{+/0}$ couple at pH 4.3 undergoes rapid electron transfer at ITO, eq 11, because the cationic character of the Ru(II) complex which provides access to the electrode double layer.[15] On the other hand, two-electron oxidation to Ru^{IV} at pH > 6, eq 12, occurs through the neutral [Ru^{IV}(bda)(L)$_2$(O)]^0/[Ru$^{III/II}$(bda)(NCMe)(L)$_2$]^0 couple resulting in slow interfacial electron transfer at ITO (Figure S4) due to the double layer effect described above.

$$i_{cat}/i_p = 0.254(k_{cat}/\nu)^{1/2} \quad (10)$$

$$[\text{Ru}^{II}(\text{MeCN})] \xrightarrow{-e^-} [\text{Ru}^{III}(\text{MeCN})]^+ (\text{pH } 4.3) \quad (11)$$

$$[\text{Ru}^{II}(\text{MeCN})]^0 + \text{H}_2\text{O} \xrightarrow{-2e^-,-2H^+} [\text{Ru}^{IV}(\text{O})]^0 + \text{MeCN} (\text{pH } 7.2) \quad (12)$$

To correct for the double layer effect at the oxide electrode in i_p/i_{cat} comparisons, experimental i_p values at the oxide were used at lower pH values under conditions where the couple was [Ru$^{III/II}$(bda)(NCMe)(L)$_2$]$^{+/0}$ and electron transfer rapid, Figure S5, Table S1. On the basis of these values, i_p/i_{cat} for water oxidation at both ITO$-$**RuP**$^{2+}$ and GC are shown plotted vs potential in Figure 8 with the variation consistent with eq 10.

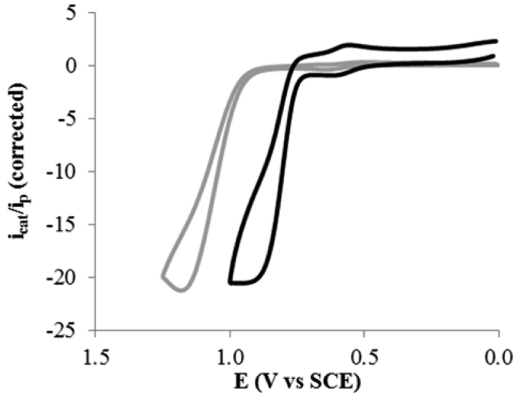

Figure 8. CVs of 0.3 mM 1 at GC (black) and ITO$-$RuP^{2+} (gray) electrodes in a pH 7.2 0.01 M phosphate-buffered solution with 10% MeCN (v/v) and 0.5 M $NaClO_4$.

On the basis of the slopes of the plots, k_{cat} = 6.8 × 10^2 at the surface-derivatized oxide, and 5.6 × 10^2 s^{-1} at GC. The agreement between these values points to electrode independent kinetics consistent with rate-limiting water oxidation following oxidation to Ru^{V}(O)$^+$. It also highlights the role of electron transfer mediation at the oxide.[11] The larger overpotential for water oxidation at ITO$-$**RuP**$^{2+}$ in Figure 8 is due to the higher potential of the relay couple with E^o = 1.07 V for ITO$-$**RuP**$^{3+/2+}$ compared to E^o = 0.78 V for the Ru$^{V/IV}$(O)$^{+/0}$ couple.

4. CONCLUSION

The absence of catalytic activity for **1** at metal oxide surfaces without an ET mediator is a significant observation. It highlights a potential limitation in the use of the Ru^{II}(bda)(L)$_2$ series in water oxidation catalysis and in photoelectrochemical applications in water splitting and CO_2 reduction at oxide surfaces.[13] We have shown here that this limitation can be overcome by use of electron transfer mediation. Mechanistically, there is also a notable difference between the surface-mediated, single-site catalytic pathway described here for **1** and the mechanism of water oxidation by Ce(IV) in acidic solutions. As shown in Scheme 2, a bimolecular coupling mechanism has been proposed for the latter.

DOI: 10.1021/acscatal.5b00720
ACS Catal. 2015, 5, 4404−4409

■ ASSOCIATED CONTENT

Supporting Information

The Supporting Information is available free of charge on the ACS Publications website at DOI: 10.1021/acscatal.5b00720.

Details of the analytical techniques, preparations and characterization data (PDF)

■ AUTHOR INFORMATION

Corresponding Author

*E-mail: tjmeyer@unc.edu (T.J.M.).

Notes

The authors declare no competing financial interest.

■ ACKNOWLEDGMENTS

This research was wholly supported by the UNC EFRC Center for Solar Fuels, an Energy Frontier Research Center funded by the U.S. Department of Energy, Office of Science, Office of Basic Energy Sciences, under Award No. DE-SC0001011.

■ REFERENCES

(1) Concepcion, J. J.; Jurss, J. H.; Brennaman, M. K.; Hoertz, P. G.; Patrocinio, A. O. T.; Murakami Iha, N. Y.; Templeton, J. L.; Meyer, T. J. *Acc. Chem. Res.* **2009**, *42*, 1954−1965.

(2) Concepcion, J. J.; Tsai, M.-K.; Muckerman, J. T.; Meyer, T. J. *J. Am. Chem. Soc.* **2010**, *132*, 1545−1557.

(3) (a) Duan, L.; Araujo, C. M.; Ahlquist, M. S. G.; Sun, L. *Proc. Natl. Acad. Sci. U. S. A.* **2012**, *109*, 15584−15588. (b) Duan, L.; Fischer, A.; Xu, Y.; Sun, L. *J. Am. Chem. Soc.* **2009**, *131*, 10397−10399.

(4) Duan, L.; Bozoglian, F.; Mandal, S.; Stewart, B.; Privalov, T.; Llobet, A.; Sun, L. *Nat. Chem.* **2012**, *4*, 418−423.

(5) Concepcion, J. J.; Zhong, D. K.; Szalda, D. S.; Muckerman, J. T.; Fujita, E. *Chem. Commun.* **2015**, *51*, 4105−4108.

(6) (a) Chen, Z.; Concepcion, J. J.; Meyer, T. J. *Dalton Trans.* **2011**, *40*, 3789−3792. (b) Tamaki, Y.; Vannucci, A. K.; Dares, C. J.; Binstead, R. A.; Meyer, T. J. *J. Am. Chem. Soc.* **2014**, *136*, 6854−6857. (c) Chen, Z.; Concepcion, J. J.; Hu, X.; Yang, W.; Hoertz, P. G.; Meyer, T. J. *Proc. Natl. Acad. Sci. U. S. A.* **2010**, *107*, 7225−7229.

(7) Vannucci, A. K.; Alibabaei, L.; Losego, M. D.; Concepcion, J. J.; Kalanyan, B.; Parsons, G. N.; Meyer, T. J. *Proc. Natl. Acad. Sci. U. S. A.* **2013**, *110*, 20918−20922.

(8) Concepcion, J. J.; Jurss, J. W.; Norris, M. R.; Chen, Z.; Templeton, J. L.; Meyer, T. J. *Inorg. Chem.* **2010**, *49*, 1277−1279.

(9) Duan, L.; Wang, L.; Inge, A. K.; Fischer, A.; Zou, X.; Sun, L. *Inorg. Chem.* **2013**, *52*, 7844−7852.

(10) Wang, L.; Duan, L.; Wang, Y.; Ahlquist, M. S. G.; Sun, L. *Chem. Commun.* **2014**, *50*, 12947−12950.

(11) Song, N.; Concepcion, J. J.; Binstead, R. A.; Rudd, J. A.; Vannucci, A. K.; Dares, C. J.; Coggins, M. K.; Meyer, T. J. *Proc. Natl. Acad. Sci. U. S. A.* **2015**, *112*, 4935−4940.

(12) Kang, R.; Chen, K.; Yao, J.; Shaik, S.; Chen, H. *Inorg. Chem.* **2014**, *53*, 7130−7136.

(13) (a) Chen, Z.; Concepcion, J. J.; Jurss, J. W.; Meyer, T. J. *J. Am. Chem. Soc.* **2009**, *131*, 15580−15581. (b) Ryan, D. M.; Coggins, M. K.; Concepcion, J. J.; Ashford, D. L.; Fang, Z.; Alibabaei, L.; Ma, D.; Meyer, T. J.; Waters, M. L. *Inorg. Chem.* **2014**, *53*, 8120−8128. (c) Gao, Y.; Zhang, L.; Ding, X.; Sun, L. *Phys. Chem. Chem. Phys.* **2014**, *16*, 12008−12013. (d) Gao, Y.; Ding, X.; Liu, J.; Wang, L.; Lu, Z.; Li, L.; Sun, L. *J. Am. Chem. Soc.* **2013**, *135*, 4219−4222. (e) Ding, X.; Gao, Y.; Zhang, L.; Yu, Z.; Liu, J.; Sun, L. *ACS Catal.* **2014**, *4*, 2347−2350. (f) Hansen, M.; Li, F.; Sun, L.; König, B. *Chem. Sci.* **2014**, *5*, 2683−2687.

(14) Norris, M. R.; Concepcion, J. J.; Glasson, C. R. K.; Fang, Z.; Lapides, A. M.; Ashford, D. L.; Templeton, J. L.; Meyer, T. J. *Inorg. Chem.* **2013**, *52*, 12492−12501.

(15) Gagliardi, C. J.; Jurss, J. W.; Thorp, H. H.; Meyer, T. J. *Inorg. Chem.* **2011**, *50*, 2076−2078.

(16) All potential values in the text are reported against SCE.

(17) (a) DuVall, S. H.; McCreery, R. L. *Anal. Chem.* **1999**, *71*, 4594−4602. (b) Lin, Q.; Li, Q.; Batchelor-McAuley, C.; Compton, R. G. *J. Phys. Chem. C* **2015**, *119*, 1489−1495.

(18) See, for example, references 4 and 7.

(19) (a) Liu, F.; Concepcion, J. J.; Jurss, J. W.; Cardolaccia, T.; Templeton, J. L.; Meyer, T. J. *Inorg. Chem.* **2008**, *47*, 1727−1752. (b) Yoshida, M.; Kondo, M.; Nakamura, T.; Sakai, K.; Masaoka, S. *Angew. Chem., Int. Ed.* **2014**, *53*, 11519−11523.

(20) (a) Concepcion, J. J.; Jurss, J. W.; Templeton, J. L.; Meyer, T. J. *Proc. Natl. Acad. Sci. U. S. A.* **2008**, *105*, 17632−17635. (b) Jurss, J. W.; Concepcion, J. C.; Norris, M. R.; Templeton, J. L.; Meyer, T. J. *Inorg. Chem.* **2010**, *49*, 3980−3982.

(21) Norris, M. R.; Concepcion, J. J.; Harrison, D. P.; Binstead, R. A.; Ashford, D. L.; Fang, Z.; Templeton, J. L.; Meyer, T. J. *J. Am. Chem. Soc.* **2013**, *135*, 2080−2083.

(22) Mulyana, Y.; Keene, F. R.; Spiccia, L. *Dalton Trans.* **2014**, *43*, 6819−6827.

(23) Young, R. C.; Keene, F. R.; Meyer, T. J. *J. Am. Chem. Soc.* **1977**, *99*, 2468−2473.

(24) (a) Li, F.; Jiang, Y.; Zhang, B.; Huang, F.; Gao, Y.; Sun, L. *Angew. Chem., Int. Ed.* **2012**, *51*, 2417−2420. (b) Duan, L.; Xu, Y.; Zhang, P.; Wang, M.; Sun, L. *Inorg. Chem.* **2010**, *49*, 209−215.

(25) During the electrolysis, a light yellow film, which was insoluble in water but soluble in organic solvents (methanol, acetonitrile), was clearly visible. The appearance of the film is due to deposition of a relatively insoluble Ru^{III} or Ru^{IV} form of the catalyst as observed previously: Jiang, Y.; Li, F.; Zhang, B.; Li, X.; Wang, X.; Huang, F.; Sun, L. *Angew. Chem., Int. Ed.* **2013**, *52*, 3398−3401.

(26) Bard, A. J.; Faulkner, L. R. *Electrochemical Methods: Fundamentals and Applications*, 2nd ed.; John Wiley & Sons, Inc.: Hoboken, NJ, 2001.

DOI: 10.1021/acscatal.5b00720
ACS Catal. 2015, 5, 4404−4409